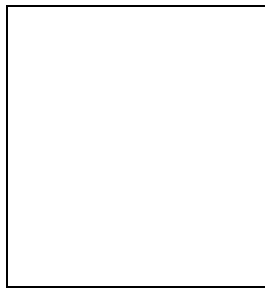


QUARTIC GAUGE BOSON COUPLINGS RESULTS AT LEP

M. MUSY
CERN



The study of charged and neutral boson vertices has been performed in different production channels at the LEP experiments. Decay rates and kinematic properties of these events are exploited to set constraints on the corresponding gauge couplings.

1 Introduction

The study of quartic gauge boson couplings (QGCs) has become possible due to the recent theoretical developments on this topic. The presence of QGCs affects the data collected for different final states at LEP. The continuous increase of the centre-of-mass energy in e^+e^- collisions allowed for the precise measurement of the W-pair cross section and couplings. Now, also the study of radiative W-pair events, $e^+e^- \rightarrow W^+W^-\gamma$, has become possible. The Standard Model (SM) predicts the existence of quartic gauge boson couplings leading to $W^+W^-\gamma$ production via *s*-channel exchange of a γ or a Z boson as shown in Fig. 1a. The contribution of these two quartic Feynman diagrams with respect to the other competing diagrams, mainly initial state radiation, is negligible at the LEP centre of mass energies. Nonetheless, the process leading to the $W^+W^-\gamma$ final state can be sensitive to anomalous contributions to the SM quartic vertices $W^+W^-\gamma\gamma$ and $W^+W^-Z\gamma$.

The theoretical framework of Ref.[¹] is used for the parametrisation of such anomalous couplings.

The existence of Anomalous QGCs would also affect the $e^+e^- \rightarrow \nu_e\bar{\nu}_e\gamma\gamma$ process via the W^+W^- fusion Feynman diagram containing the $W^+W^-\gamma\gamma$ vertex² (see Figure 1b). In the SM the reaction $e^+e^- \rightarrow \nu\bar{\nu}\gamma\gamma$ proceeds predominantly through *s*-channel Z exchange and *t*-channel W exchange, with the two photons coming from initial state radiation, whereas the SM contribution from the W^+W^- fusion is again negligible at LEP. AQGCs would enhance the $\nu\bar{\nu}\gamma\gamma$ production rate, especially for the hard tail of the photon energy distribution and for photons produced at large angles with respect to the beam direction.

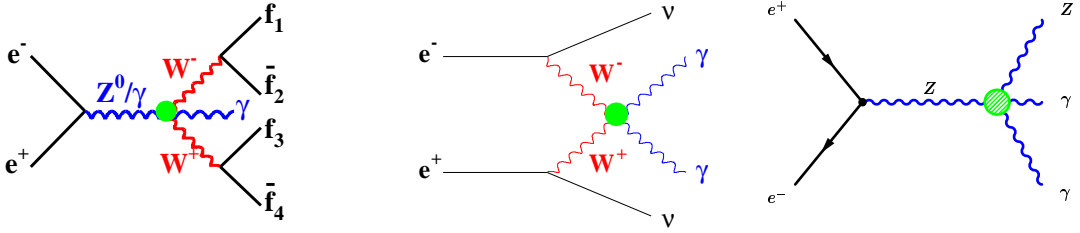


Figure 1: Feynman diagrams containing a four boson vertex leading to the (a) $W^+W^-\gamma$, (b) $\nu\bar{\nu}\gamma\gamma$, and (c) $Z\gamma\gamma$ final states.

Finally, the $Z\gamma\gamma$ production (see Fig. 1c) can also be exploited to derive limits on AQGCs, as it will be discussed in the next paragraph.

2 QGCs Analyses at LEP

Table 1 shows the different data sets used for the AQGCs analyses at LEP.

	Aleph	L3	Opal
$W^+W^-\gamma$	–	189-202 GeV	189 GeV
$\nu\bar{\nu}\gamma\gamma$	189-202 GeV	183-202 GeV	189 GeV
$Z\gamma\gamma$	–	130-202 GeV	130-208 GeV

Table 1: Data sets used for the AQGCs analyses.

The quartic couplings corresponding to reactions where two or more *charged* intermediate vector bosons are involved, are those leading to the $W^+W^-\gamma$ and $\nu\bar{\nu}\gamma\gamma$ final states.

In the $W^+W^-\gamma$ analysis, there are many Feynman diagrams leading at the $\mathcal{O}(\alpha)$ leading to the $ffff+\gamma$ final state (e.g. 142 diagrams only for $e^+e^-\rightarrow W^+W^-\gamma\rightarrow u\bar{d}e^-\bar{\nu}_e\gamma$). Anomalous contributions to the SM quartic diagrams manifest themselves through the hardening of the photon spectrum, which has the highest sensitivity with respect to the other kinematic variables in $W^+W^-\gamma$ events, and it is therefore used to extract the limits.

In the WW semileptonic and hadronic samples, an isolated photon is selected assuming different definitions for the phase space. The L3 and Opal experiments require cuts on the polar and separation angle between the photon and the charged fermions in the final state, and on the $f\bar{f}$ invariant mass (for Opal). Table 2 summarises the phase space definitions assumed.

L3	Opal
$E_\gamma > 5$ GeV	$E_\gamma > 10$ GeV
$ \cos\theta_\gamma < 0.94$	$ \cos\theta_\gamma < 0.9$
$\cos\theta_{f\gamma} < 0.94$	$\cos\theta_{f\gamma} < 0.9$
–	$\min M_{f'f} > 73$ GeV

Table 2: Phase space definition for the photon in $W^+W^-\gamma$ events.

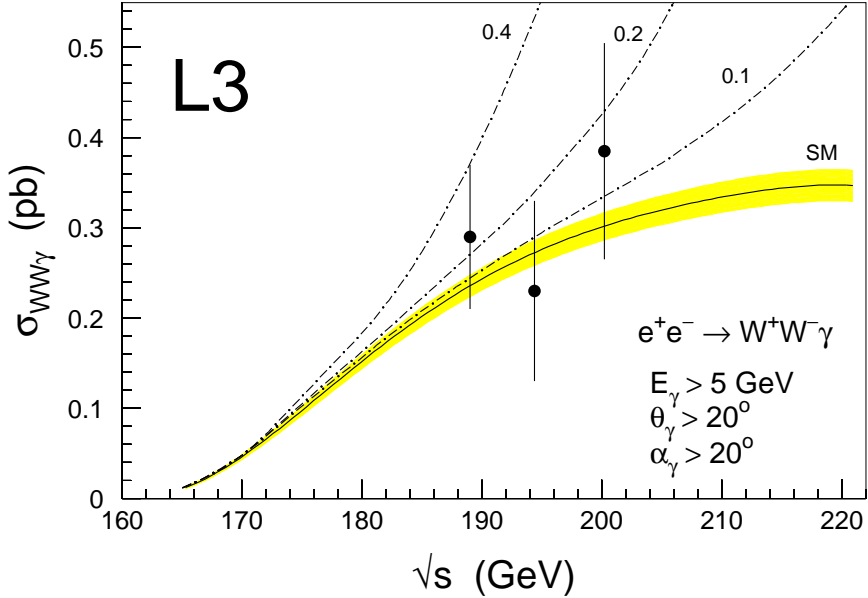


Figure 2: Measured cross section for the process $e^+e^- \rightarrow W^+W^-\gamma$.

The resulting cross sections for the L3 experiment are:

$$\begin{aligned}
 \sigma_{WW\gamma}(188.6 \text{ GeV}) &= 0.29 \pm 0.08 \pm 0.02 \text{ pb} \\
 \sigma_{WW\gamma}(194.4 \text{ GeV}) &= 0.23 \pm 0.10 \pm 0.02 \text{ pb} \\
 \sigma_{WW\gamma}(200.2 \text{ GeV}) &= 0.39 \pm 0.12 \pm 0.02 \text{ pb}
 \end{aligned}$$

while for Opal, the measurement at 189 GeV gives $\sigma_{WW\gamma} = 0.136 \pm 0.037 \pm 0.008$ pb, where the first error is statistic and the second systematic.

All the obtained results are compatible with the SM expectations.

Figure 2 shows the L3 measured cross section as a function of \sqrt{s} . The expectation band corresponds to the 5% uncertainty on the theoretical prediction from the **EEWWG**¹ Monte Carlo. The three dashed lines correspond to the cross section for non vanishing values of a_0/Λ^2 , a_c/Λ^2 , and a_n/Λ^2 (in GeV^{-2} units).

The acoplanar multi-photon channel is also sensitive to AQGCs. For a large part of the AQGC signal, the two photons recoil mass is less than the mass of the Z, while almost no SM contribution is expected in this kinematic region. Figure 3 shows the differential distribution in the specified centre-of-mass range. The **EENUNUGGANO**¹ program does not describe the effects of the SM s -channel Z exchange diagrams and the interference terms among these diagrams and the W^+W^- fusion diagram containing the $W^+W^-\gamma$ vertex. Therefore, the dashed line corresponding to the signal is not reliable over M_Z , and a recoil mass cut is applied to suppress the SM contribution.

The information from the $\nu\bar{\nu}\gamma\gamma$ total cross section, together with the information derived from the shape and normalisation of the photon spectra in $W^+W^-\gamma$ events, produces the following ADL combined limits on *charged* AQGCs using the data set of Table 1 (first two lines):

$$\begin{aligned} -0.022 \text{ GeV}^{-2} &< a_0/\Lambda^2 < 0.021 \text{ GeV}^{-2} \\ -0.043 \text{ GeV}^{-2} &< a_c/\Lambda^2 < 0.058 \text{ GeV}^{-2} \\ -0.022 \text{ GeV}^{-2} &< a_n/\Lambda^2 < 0.020 \text{ GeV}^{-2}, \end{aligned}$$

in good agreement with the SM expectation of zero for each coupling.

The Feynman diagram of Fig.1c involves only *neutral* bosons, and it is not present in the SM. Besides, as it has been recently indicated³, under more general assumptions the quartic couplings in the neutral sector, still named a_0/Λ^2 , and a_c/Λ^2 in Ref.[¹], can be regarded as independent from those in the charged sector. For this reason, on the experimental side, the convention was used to keep apart the measurements in these channels not performing any combinations, in the wait for a unified theoretical approach.

To obtain limits on AQGCs in the neutral sector, the hadronic $Z\gamma\gamma \rightarrow \text{qq}\gamma\gamma$ events are used. The signal consists in an enhancement in the rate of high energy photons, while the background mainly comes from doubly radiative returns to the Z . Figure 3 shows the $Z\gamma\gamma$ cross section as predicted by the EZGG² program^a. The same program is used to model AQGCs and to fit these couplings to the observed data distributions of $P_{T\gamma 1}$ (for L3), E_γ and $\max|\cos\theta_{\gamma i}|$ (for Opal). The following LEP combined bounds are derived⁴:

$$\begin{aligned} -0.0048 \text{ GeV}^{-2} &< a_0/\Lambda^2 < 0.0056 \text{ GeV}^{-2} \\ -0.0052 \text{ GeV}^{-2} &< a_c/\Lambda^2 < 0.0099 \text{ GeV}^{-2} \end{aligned}$$

All experimental observations are compatible with the SM predictions.

3 Conclusions

The measurements of rare processes as $Z\gamma\gamma$, $W^+W^-\gamma$ and $\nu\bar{\nu}\gamma\gamma$ constitute an important test of the SM. Preliminary results on AQGCs were presented here, including new results in the $W^+W^-\gamma$ channel up to the centre-of-mass energy of 202 GeV with a significant increase in the final precision.

References

1. J.W. Stirling and A. Werthenbach, Phys. Lett. **B446**, 369.
2. J.W. Stirling and A. Werthenbach, Eur. Phys. J. **C14** (2000) 103.
3. G. Belanger and F. Boudjema, Nucl. Phys. **B288** (1992) 201.
4. The Opal Collaboration, ICHEP abs 572 (2000), Opal PN452; The L3 Collaboration, ICHEP abs. 505 (2000), CERN-EP/2000-006.

^aThe results on $W^+W^-\gamma$ and $Z\gamma\gamma$ cross section will be reproduced on the base of a common definition for the phase space of the photon.

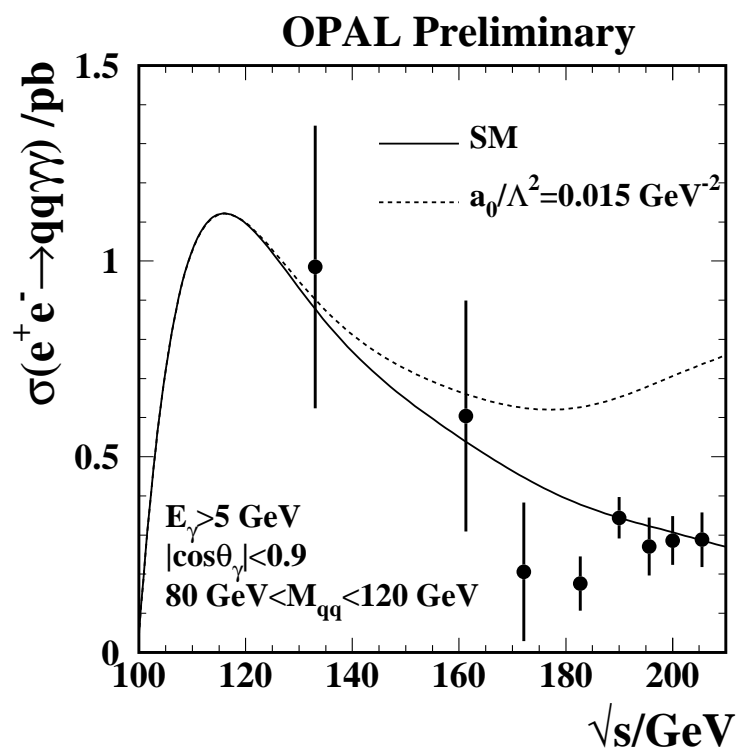
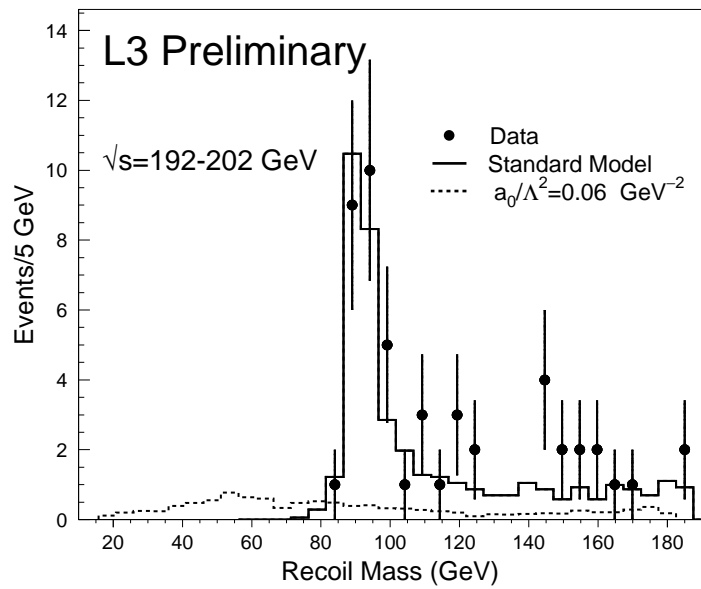


Figure 3: Cross section for the process $e^+e^- \rightarrow Z\gamma\gamma$ as a function of \sqrt{s} .